Absorption in Packed Towers with Concurrent Upward Flow

In a previous paper hydrodynamic conditions, interfacial areas and mass transfer coefficients in a packed tower with concurrent downward flows were measured. In this work a packed column with concurrent upward flow has been examined.

The results show greater area and liquid mass transfer coefficient values than with downward flow. In concurrent upward flow the increase of power consumption was less than proportional to the mass transfer increase.

The experimental data show some factors which affect the increase of area and of the liquid mass transfer coefficient.

Energy correlations of mass transfer parameters were proposed.

VITO SPECCHIA
SILVIO SICARDI
and
AGOSTINO GIANETTO

Istituto di Chimica Industriale
Politecnico di Torino, Torino, Italy

SCOPE

Previous studies done on packed towers with concurrent upward two-phase flows were concerned primarily with hydrodynamic aspects such as pressure drop and liquid saturation. Little attention has been paid to interfacial areas and internal mass transfer.

The fluid dynamic behavior was studied by Turpin (1966) in considerable detail; he limited his research, however, to only one kind of packing. The mass transfer efficiency was not studied systematically. In fact most researchers have examined this type of column only to improve the efficiency of the bubble column.

In a concurrent upward packed tower there are three main hydrodynamic regimes. At low gas flow rates, bubble flow exists; when the gas flow rate is increased, pulsing or slug flow appears and, finally for very high gas rates, spray flow results.

Different regimes have different effects on mass transfer.

This study (which employs a packed column with concurrent upward flow) is a further development of an earlier investigation on concurrent downward flow towers (Gianetto et al., 1973).

The purpose of this work was to measure interfacial areas and liquid-phase mass transfer coefficients in a packed tower with concurrent upward flow and to determine their dependence on the hydrodynamic regimes and on the various operating parameters.

Furthermore, the experimental data on hydrodynamic behavior, on interfacial areas, and on mass transfer coefficients were compared with those obtained in the previous work with concurrent downward flows.

CONCLUSION AND SIGNIFICANCE

For the same values of gas and liquid flow rates, interfacial area a, liquid mass transfer coefficient k_L, and pressure drop values in a concurrent upward packed column are always higher than those previously obtained in downflow towers.

Although the liquid holdup was not measured, the increases of a, k_L, and the pressure drop seem to be caused by this parameter. Due to gravitational force, the liquid holdup in upflow is higher than that in downflow (Turpin, 1966). This reduces the actual voidage for gas flow, resulting in a higher gas velocity and pressure drop. An increased shear stress on the liquid surface, as reflected by the pressure drop increase, would cause an entrainment of liquid in the gas phase (an increase of interfacial transfer area a) and a greater local liquid velocity on the liquid surface (an increase of surface renewal rate or mass transfer coefficient accordingly). Furthermore, owing to the gravitational force, whatever the liquid holdup, the slip velocity between the gas and liquid phases in upflow is greater than in downflow; this causes a further increase of k_L.

At a constant gas flow rate, the transfer area a for the bubble flow regime shows a small increase as the liquid flow rate increases, since a is substantially due to the number and size of the bubbles; these two parameters are probably little affected by the liquid flow rate.

The increase of a is more marked in the pulsing flow and spray flow regimes where the transfer area is mainly due to the formation of liquid droplets. In fact, some a values were larger than the geometrical packing area a_v; a values over 3 times larger than a_v were measured under some operating conditions.

When the liquid flow rate increases at constant gas flow rate, k_L shows a more marked increase in the pulsing flow regime than in bubble and spray flow. This is again due to the increase of the surface renewal rate, which in pulsing flow is higher than in the other regimes.

Correlations are proposed for a and k_L, valid in pulsing and spray flow regime, and for the various types of packing employed.

In conclusion, this study and the previous one show that the pressure drop in concurrent upward and downward columns is greater than in countercurrent columns, and consequently more power is required. Moreover, mass

transfer in concurrent columns is limited by equilibrium since no more than one single theoretical stage may be achieved.

Nevertheless, concurrent flow systems have the advantage of supporting higher throughputs, and furthermore larger interfacial areas and mass transfer coefficients can be obtained; for these reasons the application of concurrent towers in industrial processes may be of some interest, particularly for gas absorption with chemical reaction.

PREVIOUS WORK

Hydrodynamic parameters such as pressure drop and liquid saturation in a concurrent upward column were measured by Turpin (1966). He used an air-water system in columns with diameters of 50, 100, and 150 mm, packed with particles of tubular alumina of about 8 mm. He pointed out the existence of the 3 hydrodynamic regimes above and the phase velocities at which they occur.

Voyer and Miller (1968), in order to improve the gas/liquid mass transfer of the bubble columns, studied a tower with concurrent two-phase upward flow packed with meshed screen and measured the interfacial areas and the liquid mass transfer coefficients.

Mashelkar and Sharma (1970) determined the effective interfacial areas and the liquid mass transfer coefficients in a concurrent upward flow by using two types of packing.

Since these measurements were part of a study on mass transfer in bubble columns, they were not noted in detail and no reference was made to the various hydrodynamic regimes in the column.

Saada (1972) examined the interfacial areas and the liquid-phase mass transfer coefficients in a concurrent upward tower using spherical glass beads as packing; since these particles were small (0.5, 1, and 2 mm), the packing was similar to a porous bed. In fact, Saada only observed two regimes, thoroughly different from those pointed out by Turpin (1966) and also found in this study.

EXPERIMENT

The flow diagram of the equipment used is shown in Figure 1. The packed tower was of Plexiglass. Its inside diameter was 80 mm, and it could achieve a maximum height of 350 mm.

The packed test section had three suitably spaced pressure taps for determining pressure drop values and mean pressure within the test section itself.

The lower segment B of the column is illustrated in Figure 2. In this segment a series of small upright stainless steel tubes distributed the gas directly below the packing. The liquid flowed up through the holes of the upper tube-sheet. Gas-in and liquid-in samples were withdrawn from pipes *e* and *f*, respectively, placed in the segment for this purpose.

At the top of the packing, the gas was separated from the liquid in a cylindrical chamber of 140 mm inside diameter and 90 mm high. In order to avoid liquid reflux, the top of the column was at a higher level than the chamber bottom. Furthermore, to impede the entrainment of any liquid into the gas-out pipe, an inclined baffle was fitted in front of the gas exit.

The withdrawal gas sample at the end of the test section was obtained by means of a slight conical collector, with the upward central apex connected to an outlet pipe. Its opening was partially covered by a thin circular stainless steel sheet in order to reduce the entrainment of liquid droplets by the gas.

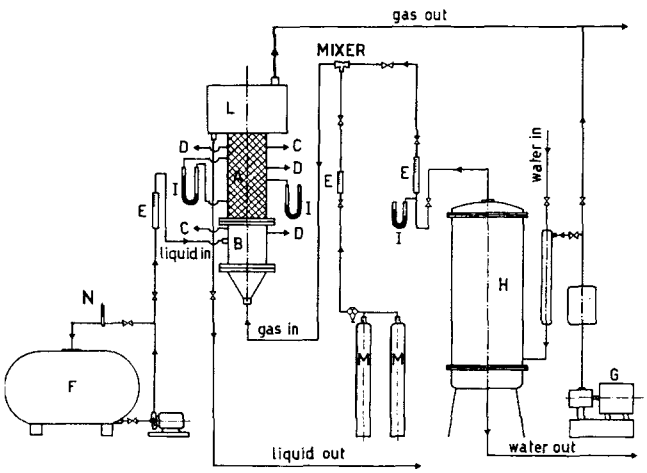

Fig. 1. Experimental apparatus: A, packing zone; B, feeding device; C, gas samples to analyzer; D, liquid samples; E, rotameters; F, liquid tank; G, blower; H, air humidifier; I, manometers; L, liquid-gas separator; M, absorbable gas bottles; N, thermometer.

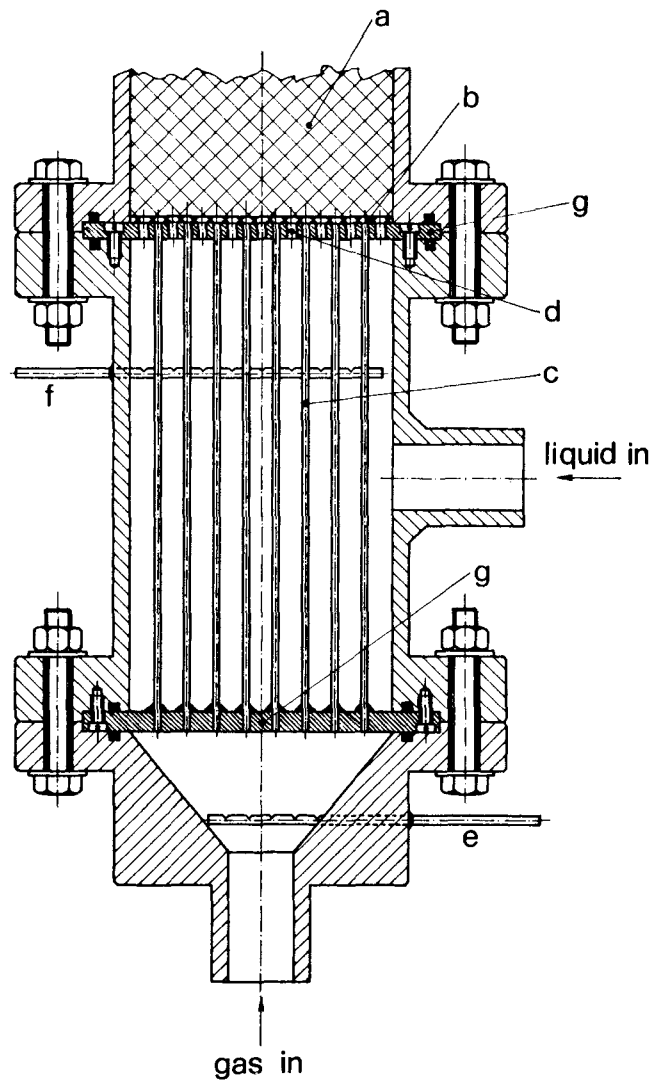

Fig. 2. Gas and liquid phase distributor: a, packing; b, net; c, gas tubes; d, liquid holes; e, gas-in withdrawal pipe; f, liquid-in withdrawal pipe; g, tube sheet.

TABLE 1. PACKING PROPERTIES

Type	Porosity ϵ	Geometrical area a_v [m^{-1}]
Glass spheres, 6 mm	0.40	595
Berl saddles, 6 mm	0.59	900
Ceramic rings, 6 mm	0.50	895

Gas samples were supplied at a constant rate to an infra-red analyzer.

The liquid-out withdrawal apparatus was comprised of a gutter 6 mm wide and 10 mm deep, which horizontally crossed the section of the column just below the gas sample device.

No liquid and gas samples were withdrawn along the test section so that no disturbance would be created in the contact zone. The influence of the end effects was tested, as will be explained later, running tests at different packing heights.

Particular care was always taken to avoid bubbling gas into the liquid samples and entrainment of liquid droplets in the gas samples, especially by controlling the withdrawal rate.

Six-mm glass spheres, 6-mm Berl saddles, and 6-mm ceramic rings were used as packing. Their geometrical properties are illustrated in Table 1.

The column was fed by a 20°C thermostatized solution. The gas phase was humidified air supplied by a rotary compressor; when necessary a soluble gas was mixed with the air.

Superficial velocities of 14 to 221 cm/s and 0.25 to 4.3 cm/s were used for the gas and liquid phases, respectively. Liquid velocities were the same as those used for the downward flow. For the gas flow lower superficial velocities (v_G = 14 cm/s and v_G = 25 cm/s) were tested in order to examine the bubble flow regime as well.

HYDRODYNAMICS

In a concurrent upflow column there are three hydrodynamic regimes. When the gas flow rate is low, whatever the liquid flow rate, there is bubble flow in which the gas phase moves in the continuous liquid phase in the form of bubbles through the channels in the packing. When the gas flow rate is increased, the interaction between the two phases increases, and this first causes alternate annular liquid and gas pistons (pulsing or slug flow) and then, with further increase in the gas flow rate, minute droplets of liquid suspended in the gas phase (spray flow), while part of the liquid flows over the packing as a film.

The hydrodynamic regime limits of the bubble flow, pulsing or slug flow and spray flow observed in this work were compared with those obtained by Turpin (1966).

In Figure 3 the results we obtained with 3 types of packing are compared with Turpin's using the same graphical presentation.

Only a small zone of the various fields coincides in these diagrams. An explanation of the discrepancy, particularly the reversal in slug and spray flow, is very difficult since we have only a unilateral view of the experiments; as a conjecture some importance may be attached to the different physical properties of the liquid phases used (water by Turpin and NaOH solutions by us); moreover, a different method was adopted for supplying the two phases, hence obtaining a different degree of dispersion of the two phases at the inlet of the packing. In fact, in Turpin's experiments the liquid and gas feed were brought together in a 2-in. tee, and the combined flow was then passed through a stainless steel wire mesh filter to distribute the phases uniformly across the column section.

Figure 4 compares upflow pressure drop vs. v_L with those obtained in the previous study with a concurrent downward column (Gianetto et al., 1973). The comparison has been made for different gas flow rates and for all the packing used.

The experimental upflow points are always higher than the downflow points. This is probably due to the effect of gravitational force and of the higher values of the hold-up in the upflow.

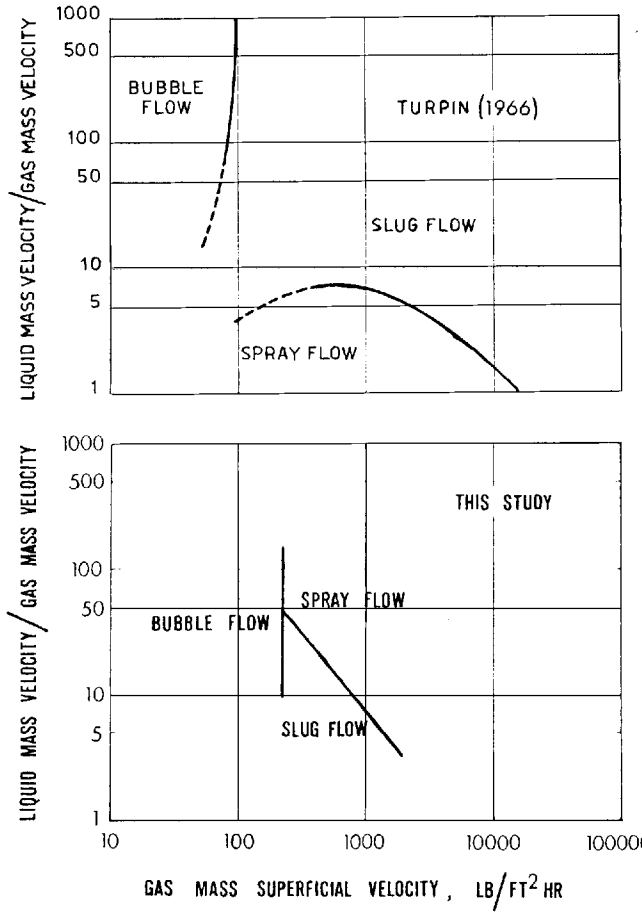

Fig. 3. Hydrodynamic regimes observed by Turpin (1966) and in our study.

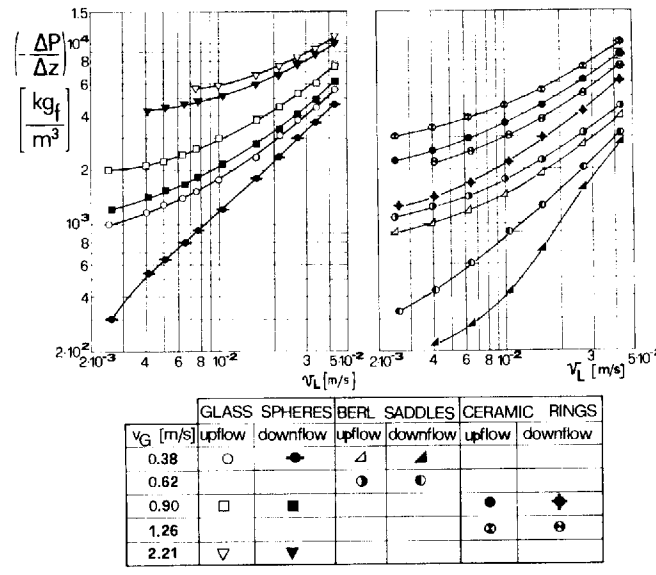

Fig. 4. Upflow and downflow pressure drops vs. v_L, for different v_G, for all the packing.

INTERFACIAL AREAS

The interfacial areas were measured by chemical absorption of CO_2 in NaOH solutions; CO_2 was mixed with air at 5 to 6% in volume; the conditions of fast and pseudo first-order reaction were satisfied (Danckwerts and Sharma, 1966).

The CO_2 absorption data were obtained with an infrared gas analyzer and verified by means of mass balances on the basis of liquid analyses by titration (the mass balances agreed to within 10%).

As for downflow measurements 2, 1, and 0.5 N aqueous solutions of sodium hydroxide were employed; sodium sulphate was added, when necessary, in order to maintain the same values of physical liquid properties for all the experiments.

When the absorbent liquid was a solution of pure NaOH, the absorbed CO_2 was measured by titration with HCl of the residual sodium hydroxide, after precipitation of the carbonates by $BaCl_2$. In the presence of Na_2SO_4, CO_2 was determined by titration of bicarbonates, with HCl, at low temperature, in the pH range between the color change of phenolphthalein and methyl orange.

The mean value in the column of the overall mass transfer coefficient K_ya, in the presence of chemical reaction, was calculated by the following equation:

$$K_ya = \frac{G_m}{S\,Z} \ln \frac{y_{in}}{y_{out}} \qquad (1)$$

with the plug flow assumption for the two phases; y_{in} and y_{out} are the CO_2 molar fraction in gas phase at the inlet and the outlet of the test section respectively.

The overall mass transfer resistance was expressed as the addition of the gas phase and the liquid phase mass transfer resistance

$$\frac{1}{K_ya} = \frac{1}{k_ya} + \frac{1}{am\sqrt{\mathcal{D}\,k_r\,[OH^-]_m}} \qquad (2)$$

The values of the kinetic constant k_r of the reaction between the absorbed CO_2 and hydroxyl ions in the liquid phase at 20°C as a function of the various ion species present in the solution were taken from the work by Pinsent et al. (1956).

The CO_2 solubility values m were determined by the method of Van Krevelen and Hoftijzer (1948), in which allowance was made for ionic strength and checked with those by Nijsing et al. (1959).

The liquid-phase CO_2 diffusivity $\mathcal{D}$ was calculated using the results of Nijsing et al. (1959), obtained with various solutions, by the following equation:

$$\frac{\mathcal{D}\mu_L}{T} = 5{,}8 \cdot 10^{-15} \frac{\text{kg m}}{\text{s}^2\ ^\circ\text{K}} \qquad (3)$$

The mean hydroxyl ion concentrations $[OH^-]_m$ were calculated arithmetically on the basis of the inlet and outlet concentrations.

As stated in Equation (2), plotting $1/K_ya$ vs. $1/m\sqrt{\mathcal{D}k_r[OH^-]_m}$, straight lines of intercept $1/k_ya$ and slope $1/a$ were obtained. In Figure 5 this plot of experimental points for $v_G = 0.38$ m/s, at various v_L values, is shown; each set of points is satisfactorily arranged on a straight line.

Regarding the fact that the chemically determined area may be greater than that connected with physical absorption (Joosten and Danckwerts, 1973), the high gas-liquid interaction in upward concurrent absorbers notably reduces the difference between the values of these areas by limiting the importance of dead pockets for transfer purposes. Moreover, the chemical method is now the only one available for this type of measurement.

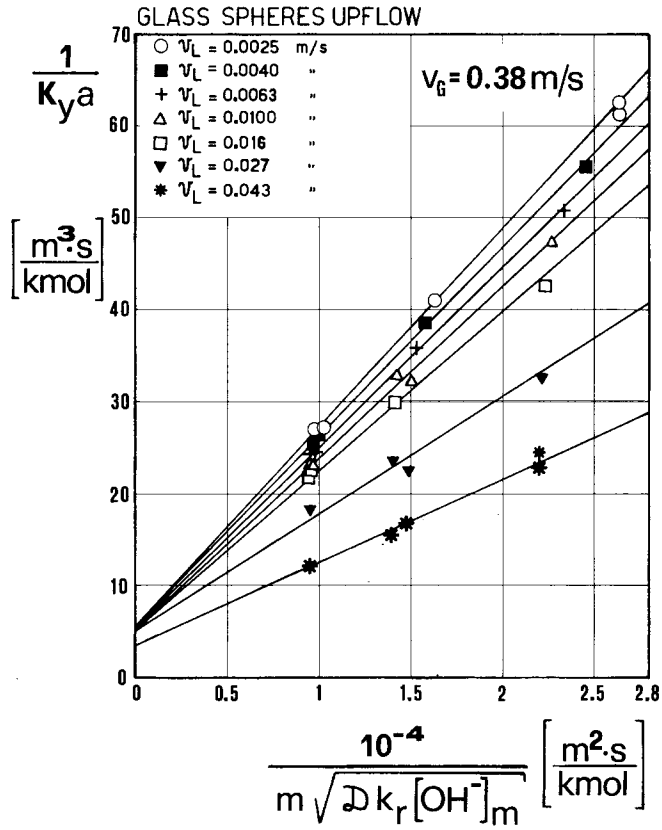

Fig. 5. Plot of $1/K_ya$ vs. $1/m\sqrt{\mathcal{D}k_r[OH^-]_m}$ for glass spheres

The mean overall mass transfer coefficient K_ya for a given gas flow rate and for glass spheres was measured for two different packing heights (320 mm and 160 mm). A test was also run varying the inlet CO_2 from 5.5% to 9%. In both cases only very slight variations of K_ya, about ± 5%, were observed. This demonstrated that end effects had no considerable influence on K_ya.

In Figure 6 solid lines show the behavior of the ratio between the measured transfer area and the geometrical area a/a_v vs. v_L with glass sphere packing; dotted lines indicate, for the same liquid and gas flow rates, the values for concurrent downward flows (Gianetto et al., 1970). Moreover, for a/a_v values in downflow there is also the f line which shows the beginning of the pulsing flow regime. The lines concerning $v_G = 0.25$ m/s and $v_G = 0.14$ m/s for upflow refer to the bubble-flow regime. The upflow values are higher than the downflow ones, but the differences, v_G being equal, diminish with the increase in liquid rate as previously observed for the pressure drops. This behavior is probably due to the fact that at low liquid rates the gas-liquid interaction is more reduced in downflow absorbers while, for functional reasons, the interaction is already quite marked in upflow absorbers. It tends to assume high values in those regimes where both types of absorbers work with high flow rates.

Furthermore it is notable that, for not excessively low flow rates, the values of a found for each type of packing were higher than the geometrical packing area a_v; some values were three times greater than a_v. This was due to a very high two-phase dispersion in the packing channels.

The trend of a/a_v vs. v_L is similar to that observed by Saada (1972); the values determined by this author were, however, much lower—probably because he used packing of very small dimensions.

As for the downflow interfacial areas, a/a_v values could

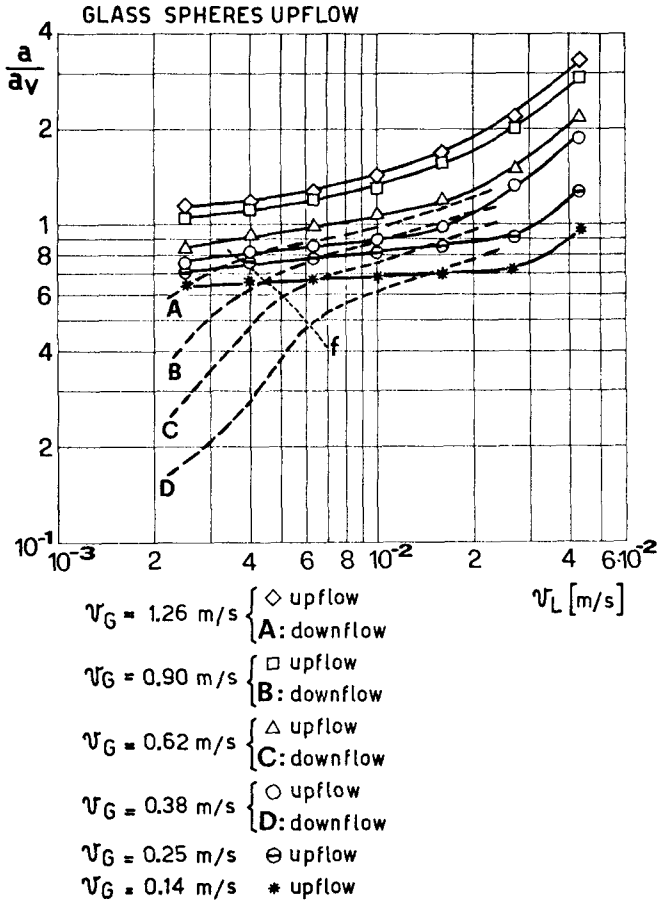

Fig. 6. Ratio between the interfacial and geometrical area a/a_v vs. v_L for the glass spheres; the line f is the lower limit for pulsing flow in downward operation.

be correlated as a function of $(-\Delta P/\Delta z)\ \epsilon/a_v$; this correlation is valid only in pulsing and spray flow regimes.

In fact, in these regimes the interfacial area is mainly due to droplet formation which is connected to the dissipated energy in the column. The area also depends on the free volume of the tower in which the entrained droplets can move. For this reason the correlation must allow for the dissipated energy: $(-\Delta P/\Delta z)$: and the geometrical characteristics of the packing: ϵ/a_v, which is proportional to the packing's hydraulic diameter.

This correlation is shown in Figure 7.

In this figure the interpolation line of the downflow data is also shown (Gianetto et al., 1970).

The upflow analytical correlation with a relative mean quadratic error of 6.2% is

$$\frac{a}{a_v} = 0.29\left[\left(-\frac{\Delta P}{\Delta z}\right)\frac{\epsilon}{a_v}\right]^{1.17} + 0.61 \qquad (4)$$

The two lowest gas flow rates: $v_G = 14$ cm/s and $v_G = 25$ cm/s experimented with glass sphere packing, could not be correlated as the gas continuous flow and rippled flow regimes for downflow. This was because the characteristic regime for low gas rates is mainly of the bubbling type, and the transfer area is therefore not substantially due to formation of liquid droplets.

MASS TRANSFER WITH CONTROLLING RESISTANCE IN LIQUID PHASE

Mass transfer coefficients in the liquid phase were measured by oxygen desorption with air from a 2N solution of caustic soda (the same used in the area measurements), previously saturated with O_2 to a p_{O_2} value of about 500 to 550 mmHg.

Since O_2 is poorly soluble in the liquid, the transfer resistance is virtually confined to this phase.

Polarographic analysis was done on the liquid phase at the inlet and outlet of the test section with a continuous analyzer whose calibration was systematically checked. Particular care was taken to prevent pressure and temperature fluctuations in the measuring cells.

No useful analysis could be made of the gas phase due to the extremely small variation in its O_2 content.

k_La ($\simeq K_La$) was calculated by the following differential equation:

$$-L\left(\frac{dc_{O_2}}{dz}\right) = k_La\ S(c_{O_2} - c^*_{O_2}) \qquad (5)$$

assuming plug flow for both phases. In fact only very slight k_La variations, on the order of experimental errors, result from taking axial dispersion into account as it was shown by Mashelkar and Sharma (1970), using for their calculations the axial dispersion coefficients obtained by Carleton et al. (1969).

The differential Equation (5) was integrated numerically between the inlet and outlet of the test section and k_La determined by trial and error until the final concentration in the liquid, as calculated for $z = Z$, was equal to the observed experimental value. Henry's law of gas-liquid equilibrium was assumed to be valid and note was also made of a linear variation of total pressure along the column since this had an appreciable effect on the value of the driving force.

It was also found, for glass sphere packing, that increases of about 50% in the height of the packing as well as 30% of the O_2 dissolved in the liquid feed caused variations in the k_La values of ± 8%.

The agreement of the results varying the height of the test section showed that the end effects had no considerable influence on k_La.

Figure 8 shows the behavior of k_La vs. v_L and v_G for the glass spheres. The k_La values are always higher than the downflow values obtained in the previous work (Gianetto et al., 1973). Furthermore, the increase in k_La observed as liquid rate increases is about 1/5 of that found in the downflow operation.

In Figure 9 k_La is plotted vs. the energy dissipated in

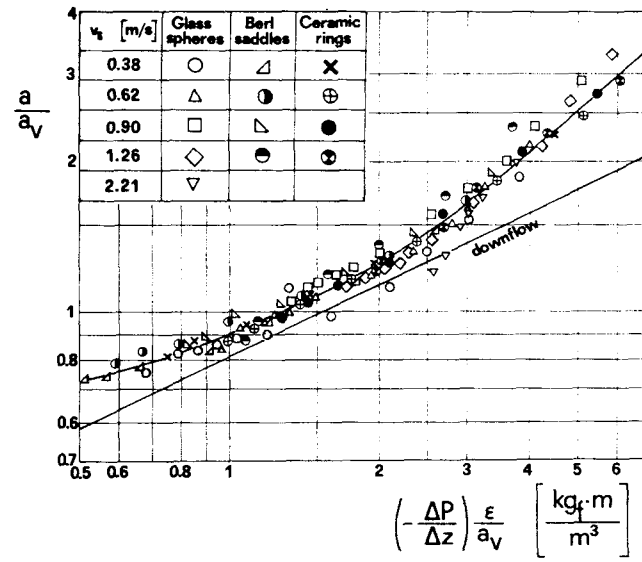

Fig. 7. Correlation of a/a_v vs. $(-\Delta P/\Delta z)\ \epsilon/a_v$.

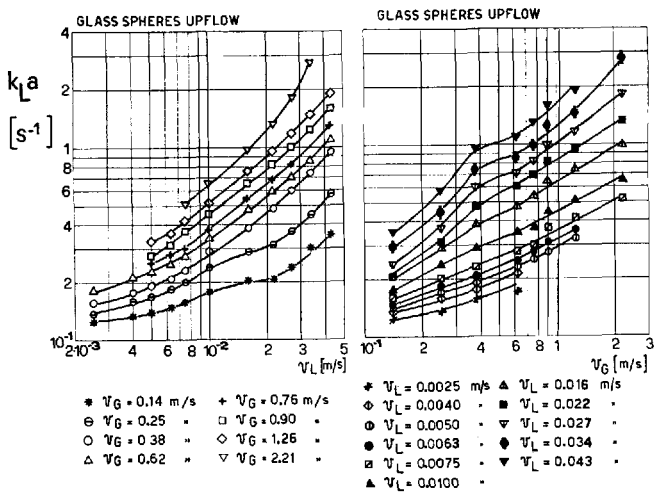

Fig. 8. k_La vs. v_L for various v_G and vice versa, using glass sphere packing.

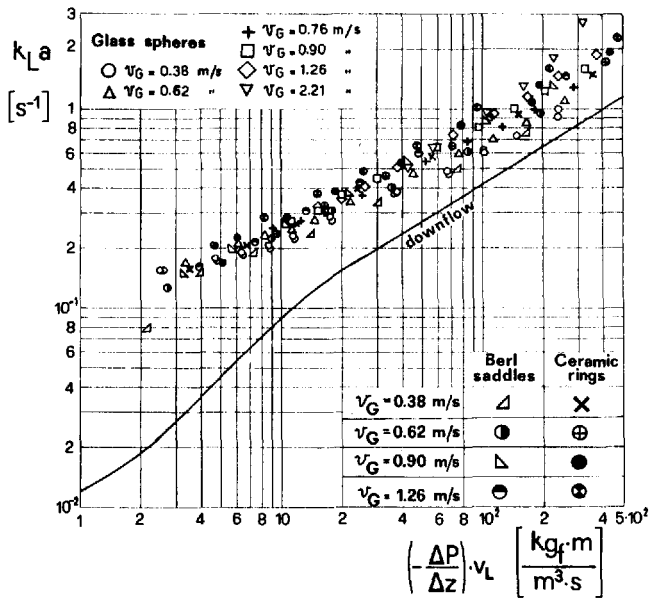

Fig. 9. k_La vs. the energy dissipated in liquid phase $(-\Delta P/\Delta z)\, v_L$.

the tower by the liquid phase $(-\Delta P/\Delta z)\, v_L$, according to Reiss' correlation for downflow (1967): the upflow values of k_La are on the average 100% greater than the downflow values. As in the previous area correlation, the values of k_La for the two lowest gas rates for glass spheres (bubbling regime), could not be correlated.

Figure 10 shows the ratio between k_La in upflow and downflow for the same gas and liquid flow rates, vs. the ratio between the dissipated energy for the two-phase flow resistance on the packing $(-\Delta P/\Delta z)\,(v_G + v_L)$ in upflow and downflow.

In energy evaluation, variation of the kinetic energy in the two phases between inlet and outlet of the packing was not taken into account because it was very difficult to determine this parameter without measuring hold-up. Moreover, preliminary tests showed that it had only a limited and not constant influence on the mass transfer; in fact, the loss of kinetic energy between inlet and outlet has different importance on the total loss of energy in the column according to the height of the packing section.

For the upflow operation the increase in k_La is always greater than the corresponding increase in dissipated energy, especially for low liquid and gas flow rates, that is, for high values of abscissa. This result is important because energy consumption is the main criterion for choosing concurrent equipment.

Figure 11 shows the plot of k_L vs. v_L for the glass spheres for various gas flow rates in upflow and in downflow. The k_L value is very little influenced by the gas flow rate and moderately affected by the liquid rate; Saada (1972) furthermore found k_L independent of these two parameters.

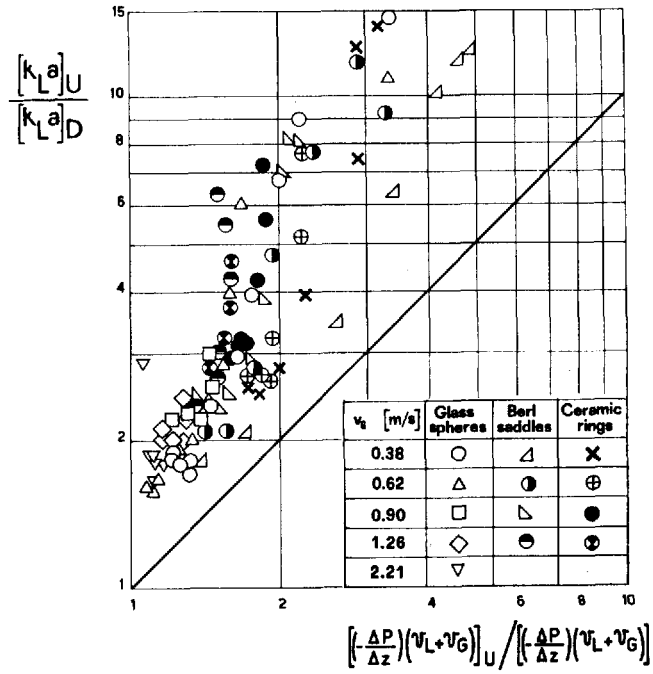

Fig. 10. Ratio between k_La in upflow and downflow vs. the ratio between $(-\Delta P/\Delta z)\,(v_G + v_L)$ in upflow and downflow.

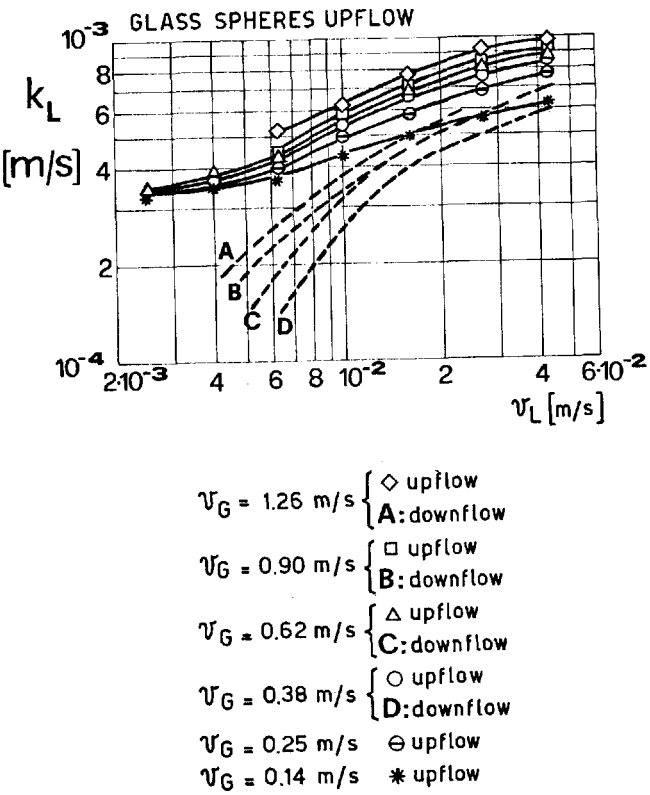

Fig. 11. k_L vs. v_L for various gas flow rates and for the glass spheres.

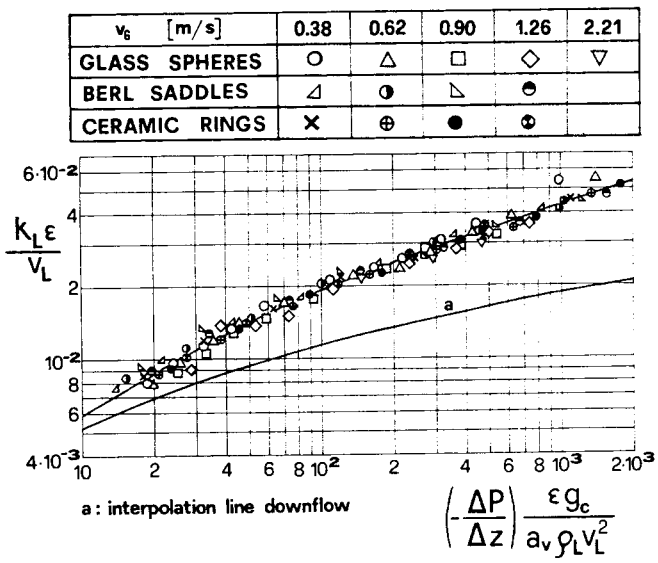

Fig. 12. $k_L\epsilon/v_L$ vs. $(-\Delta P/\Delta z)\, g_c\epsilon/a_v\rho_L v^2_L$.

The upflow k_L values are higher than the downflow ones, the differences diminishing as v_L increases when v_G is constant. This behavior is similar to that observed for the transfer area and may be attributed to the same causes.

As in the case of downflow, Figure 12 shows the values of the Sherwood number $k_L\epsilon/v_L$ for all the packings, in pulsing and spray flow regimes, vs. the parameter

$$\left(-\frac{\Delta P}{\Delta z}\right)\frac{g_c\epsilon}{a_v\rho_L v_L{}^2},$$

which represents the ratio between dissipated energy and that absorbed by the liquid phase (Gianetto et al., 1973).

It was noted that the points relating to the low gas flow rates in bubble flow regime adapted well to this correlation. However, since no acceptable physical justification could be found, it was decided to exclude these points, from Figure 12 as well, as was done with the previous ones.

The interpolation formula for the experimental data

$$10^3\frac{k_L\epsilon}{v_L} = 7.96\left[\left(-\frac{\Delta P}{\Delta z}\right)\frac{g_c\epsilon}{a_v\rho_L v^2_L}\right]^{0.275} - 9.41 \quad (6)$$

gives a relative mean quadratic error of 7.8%.

The values of $k_L\epsilon/v_L$, v_G being equal are greater in upflow than those corresponding in downflow, mainly at low liquid rates (right-hand side of the figure); but they approach downflow values as liquid flow rate increases.

Finally, Figures 7 and 12, respectively illustrating the behavior of a/a_v and $k_L\epsilon/v_L$ vs. the energy parameters, give some indication of the contribution of the factors a and k_L in the product k_La. Figure 7 in fact shows that a values are increased in upflow for high energy dissipation; in Figure 12, with respect to k_L, the advantage takes place for high ratios between total dissipated energy and kinetic energy in the liquid.

In conclusion, the higher value of a in upflow than in downflow is a result of the greater pressure drops and consequently of the greater dispersion of the liquid in the gas phase; the advantage of k_L for slower liquid velocities is probably due to the increase in circulation inside the liquid drops caused, among other things, by the greater slip velocity between the liquid and gas phase.

ACKNOWLEDGMENTS

Research was financed by the Consiglio Nazionale delle Ricerche. Thanks are due to Mr. Paolo Diano for his mechanical assistance.

NOTATION

a = interfacial area per unit volume of column, m^{-1}
a_v = geometrical area per unit volume of column, m^{-1}
c_{O_2} = O_2 concentration in liquid phase, kmoles/m^3
$c^*_{O_2}$ = O_2 concentration in liquid phase in equilibrium with gas phase, kmoles/m^3
$\mathcal{D}$ = CO_2 diffusivity in liquid phase, m^2/s
G_m = mean molar gas rate, kmoles/s
g_c = conversion factor, $kg_m \cdot m/kg_f \cdot s^2$
K_y, k_y = overall and gas phase mass transfer coefficients with chemical reaction, kmoles/m^2s
K_L, k_L = overall and liquid phase mass transfer coefficients m/s
k_r = kinetic constant of reaction between dissolved CO_2 and hydroxyl ion in liquid phase, m^3/kmoles · s
L = liquid flow rate, m^3/s
m = solubility coefficient of CO_2 in liquid phase, kmoles/m^3
$[OH^-]_m$ = mean concentration of hydroxyl ion in the column, kions/m^3
$\left(-\frac{\Delta P}{\Delta z}\right)$ = pressure drop, kg_f/m^3
S = section of the column, m^2
T = absolute temperature, °K
v_G = superficial velocity of the gas phase, m/s
v_L = superficial velocity of the liquid phase, m/s
Z = packing height, m
z = distance from the bottom of the packing, m
y_{in} = molar fraction of CO_2 at the inlet of the test section, dimensionless
y_{out} = molar fraction of CO_2 at the outlet of the test section, dimensionless

Greek Letters

ϵ = packing porosity, dimensionless
μ_L = liquid phase viscosity, kg/ms
ρ_L = liquid phase density, kg/m^3

LITERATURE CITED

Carleton, A. T., R. J. Flain, J. Rennie, and F. H. H. Valentin, "Some Properties of a Packed Bubble Column," *Chem. Eng. Sci.*, **22**, 1839 (1967).

Danckwerts, P. V., and M. M. Sharma, "The Absorption of Carbon Dioxide into Solutions of Alkalis and Amines," *Trans. Inst. Chem. Eng.*, **44**, CE244 (1966).

Gianetto, A., G. Baldi, and V. Specchia, "Absorption in Packed Tower with Concurrent Downward High-Velocity Flow—I: Interfacial Areas," *Quad. Ing. Chim. Ital.*, **6**, 125 (1970).

Gianetto, A., V. Specchia, and G. Baldi, "Absorption in Packed Tower with Concurrent Downward High-Velocity Flow—II: Mass Transfer," *AIChE J.*, **19**, 916 (1973).

Joosten, G. E. H., and P. V. Danckwerts, "Chemical Reaction and Effective Interfacial Areas in Gas Absorption," *Chem. Eng. Sci.*, **28**, 453 (1973).

Mashelkar, R. A., and M. M. Sharma, "Mass Transfer in Bubble and Packed Bubble Columns," *Trans. Inst. Chem. Eng.*, **48**, 162 (1970).

Nijsing, R. A. T. O., R. H. Hendriks, and H. Kramers, "Absorption of CO_2 in Jets and Falling Films of Electrolyte Solutions, with and without Chemical Reaction," *Chem. Eng. Sci.*, **10**, 88 (1959).

Pinsent, B. R. W., L. Pearson, and F. J. W. Roughton, "The Kinetics of Combination of Carbon Dioxide with Hydroxide Ions," *Trans. Faraday Soc.*, **52**, 1512 (1956).

Reiss, L. P., "Cocurrent Gas-Liquid Contacting in Packed Columns," *Ind. Chem. Eng. Process Design Develop.*, **6**, 486 (1967).

Saada, N. Y., "Assessment of Interfacial Area in Cocurrent Two-Phase Flow in Packed Beds," *Chim. Ind. Genié Chimique*, **105**, 1415 (1972).

Turpin, J. L., "Prediction of Pressure Drop for Two-Phase, Two-Component Cocurrent Flow in Packed Beds," Ph.D. thesis, Univ. Oklahoma, Norman (1966).
Van Krevelen, D. W., and P. J. Hoftijzer, "Sur la Solubilité des Gas dans les Solutions aqueuses," *Chim. Ind., XXIeme Cong. Int. Chim. Ind.*, 168 (1950).
Voyer, R. D., and A. I. Miller, "Improved Gas-Liquid Contacting in Concurrent Flows," *Can. J. Chem. Eng.*, 46, 335 (1968).

Manuscript received October 23, 1973; revision received February 12 and accepted February 13, 1974.

Influence of Crystal Size on the Rate of Contact Nucleation in Stirred-Tank Crystallizers

The purpose of this study was to investigate the influence of seed crystal size on the rate of nucleation in batch stirred-tank crystallizers. Experimental results confirm the existence of such an effect. Nucleation rate data are correlated with a second-order polynomial in seed crystal size; coefficients of the correlation are functions of the solute-solvent system, crystallizer geometry, and mixing conditions. The empirical correlation is incorporated into a population balance model for determining the nucleation rate in multi-seed crystallizers. The observed results are explained in terms of variations in impact energy, circulation frequency, and target efficiency.

L. G. BAUER
R. W. ROUSSEAU
and
W. L. McCABE

Department of Chemical Engineering
North Carolina State University
Raleigh, North Carolina 27607

SCOPE

Secondary crystal nucleation is defined as the formation of crystals in the presence of growing seed crystals—the condition under which most industrial crystallizers operate. Contact nucleation, a subset of secondary nucleation, is defined as the formation of crystals as a result of the collision of a seed crystal with a solid object. Pioneering work on contact nucleation by Clontz and McCabe (1971) and Johnson, Rousseau, and McCabe (1972) has demonstrated that an increase in impact energy results in an increase in the number of nuclei formed as a result of that impact. Furthermore, Ottens and DeJong (1972), showed that the primary source of contact nucleation in stirred-tank crystallizers is the collision of seed crystals with the impeller. When these observations were considered together, it was believed that a variation in impact energy within stirred-tank crystallizers could result from a variation in seed crystal size as well as impeller speed.

However, previous stirred-tank studies on contact nucleation had been conducted in crystallizers whose product streams, and necessarily the in-tank liquor, contained distributions of crystal sizes. Such systems made it difficult to isolate the effect of seed crystal size on the contact nucleation rate from existing data. Therefore, an experimental program was developed to observe and correlate this phenomenon. With the results of this study a better understanding of the variables affecting contact nucleation in batch and continuous stirred-tank crystallizers is to be achieved. Furthering the state of knowledge in this area will lead to better nucleation control in systems where excessive in insufficient nucleation is of concern.

CONCLUSIONS AND SIGNIFICANCE

The influence of seed crystal size on the nucleation rate in batch stirred-tank crystallizers has been demonstrated. Nucleation rates were correlated with seed crystal size at various stirrer speeds and at fixed supersaturation and crystallizer geometry. Expressing the size-dependent nucleation rate as $B_L{}^0\left[\dfrac{\text{nuclei generated}}{(\text{time})(\text{volume})(\text{seed crystal})}\right]$ and the population density as $n\left(\dfrac{\text{number of seed crystal}}{(\text{volume})(\text{size})}\right)$, a model was proposed for incorporating the size-dependent nucleation rate into the determination of an overall nucleation rate for multi-seed crystallizers:

$$B^0 = \int_0^\infty B_L{}^0\, ndL$$

Correspondence concerning this paper should be addressed to R. W. Rousseau. L. G. Bauer is with the Chemical Engineering Department, South Dakota School of Mines and Technology, Rapid City, South Dakota 57701.